Supplement of Biogeosciences, 17, 5721–5743, 2020
https://doi.org/10.5194/bg-17-5721-2020-supplement

Biogeosciences Open Access EGU

Supplement of

Evaluating two soil carbon models within the global land surface model JSBACH using surface and spaceborne observations of atmospheric CO_2

Tea Thum et al.

Correspondence to: Tea Thum (tthum@bgc-jena.mpg.de)

S1 Details on JSBACH simulations

Simulations were conducted on Mistral (the High Performance Computing system of the German Climate Computing Center (DKRZ)), using revision 8522 of $cosmos-landveg\_rc-echam6.3\_FOM-alloc$, a svn branch of cosmos-landveg, the former JSBACH development branch of the department "The Land in the Earth System" of the Max Planck Institute for Meteorology.

For each of the two transient simulations described in the main text, an own spin-up has been conducted. Both spin-ups follow the same set-up, cycling detrended 1901-1920 forcing based on CRUNCEP v6 with a constant 1860 CO_2 concentration (286.42 ppm). The spin-ups used a static land-use map for 1860, based on 1860 crop and pasture cover from the LUHv1 dataset (Hurtt et al., 2011) and a potential vegetation map extrapolated from remote sensing (Pongratz et al., 2008).

References

Hurtt, G. C., Chini, L. P., Frolking, S., Betts, R. A., Feddema, J., Fischer, G., Fisk, J. P., Hibbard, K., Houghton, R. A., Janetos, A., Jones, C. D., Kindermann, G., Kinoshita, T., Klein Goldewijk, K., Riahi, K., Shevliakova, E., Smith, S., Stehfest, E., Thomson, A., Thornton, P., van Vuuren, D. P., and Wang, Y. P.: Harmonization of land-use scenarios for the period 1500–2100: 600 years of global gridded annual land-use transitions, wood harvest, and resulting secondary lands, Climatic Change, 109, 117, https://doi.org/10.1007/s10584-011-0153-2, https://doi.org/10.1007/s10584-011-0153-2, 2011.

Pongratz, J., Reick, C., Raddatz, T., and Claussen, M.: A reconstruction of global agricultural areas and land cover for the last millennium, Global Biogeochemical Cycles, 22, https://doi.org/10.1029/2007GB003153, https://agupubs.onlinelibrary.wiley.com/doi/abs/10.1029/2007GB003153, 2008.

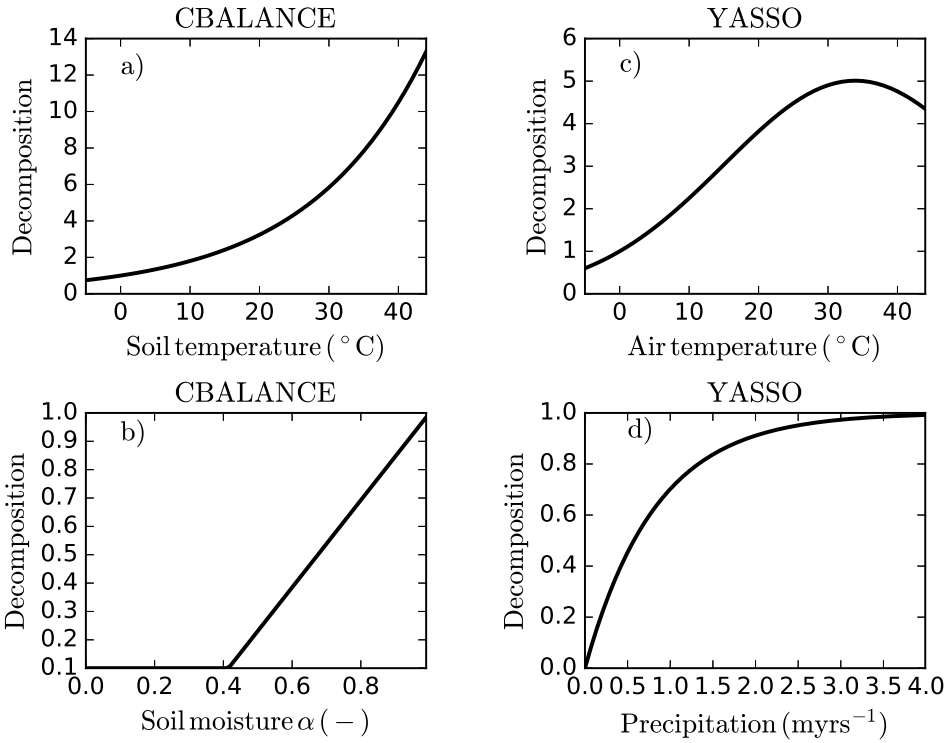

Figure S1. The environmental response functions of CBALANCE (CBA) and YASSO (YAS) models. The dependency on soil temperature by CBA (a), on soil moisture by CBA (b), on air temperature by YAS (c) and on precipitation by YAS (d).

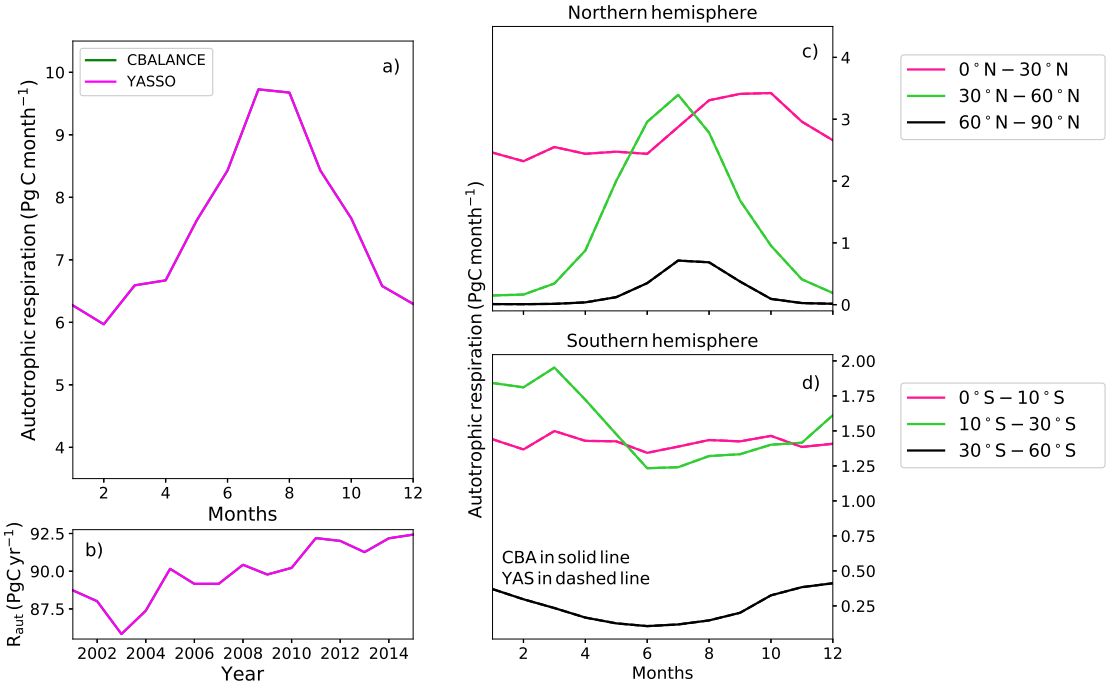

Figure S2. The global seasonal cycle (a), annual values (b), and seasonal cycle in different latitudinal zones in Northern (c) and Southern (d) Hemispheres of the autotrophic respiration (R_{aut}), which is independent of the soil module (therefore, the lines for CBA and YAS overlap in this figure).

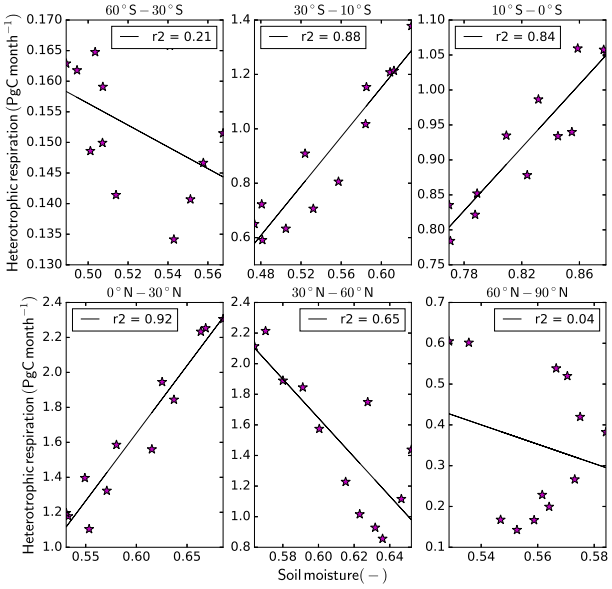

Figure S3. The monthly heterotrophic respiration from the CBALANCE model as a function of soil moisture (α) for different latitudinal regions.

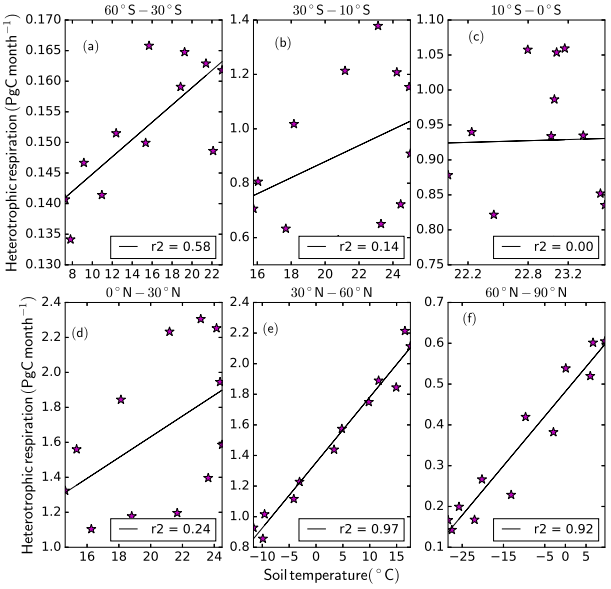

Figure S4. The monthly heterotrophic respiration from the CBALANCE model as a function of soil temperature for different latitudinal regions.

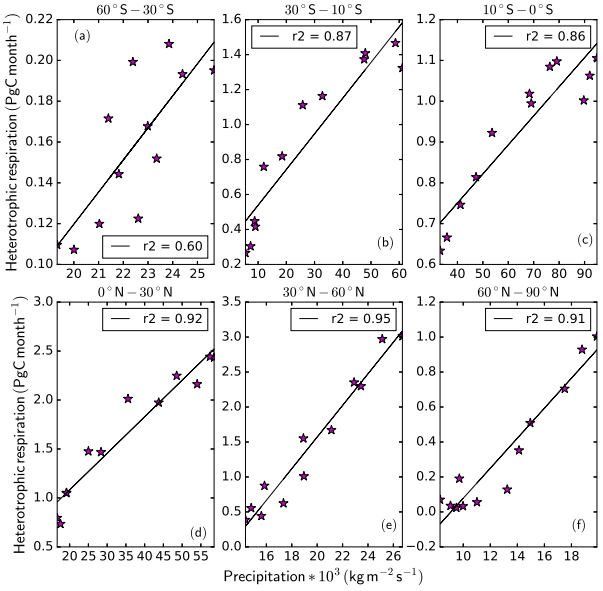

Figure S5. The monthly heterotrophic respiration from the YASSO model as a function of precipitation for different latitudinal regions.

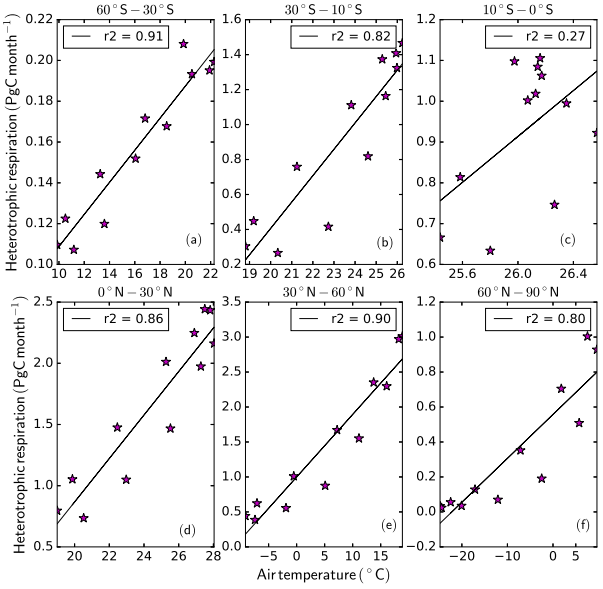

Figure S6. The monthly heterotrophic respiration from the YASSO model as a function of air temperature for different latitudinal regions.

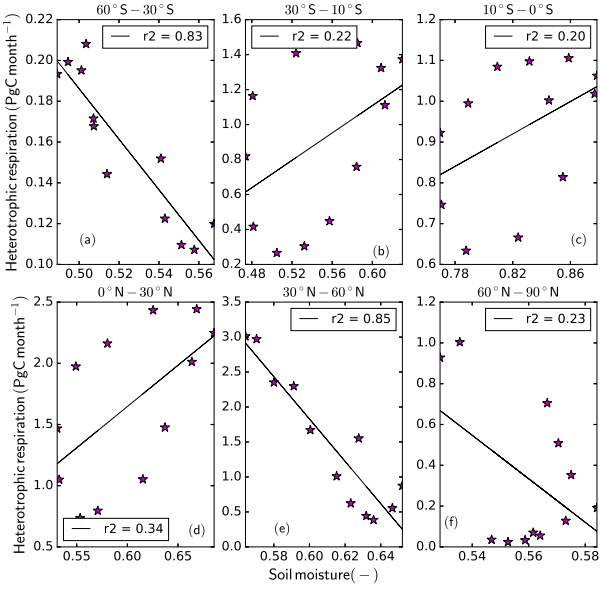

Figure S7. The monthly heterotrophic respiration from the YASSO model as a function of soil moisture (α) for different latitudinal regions.

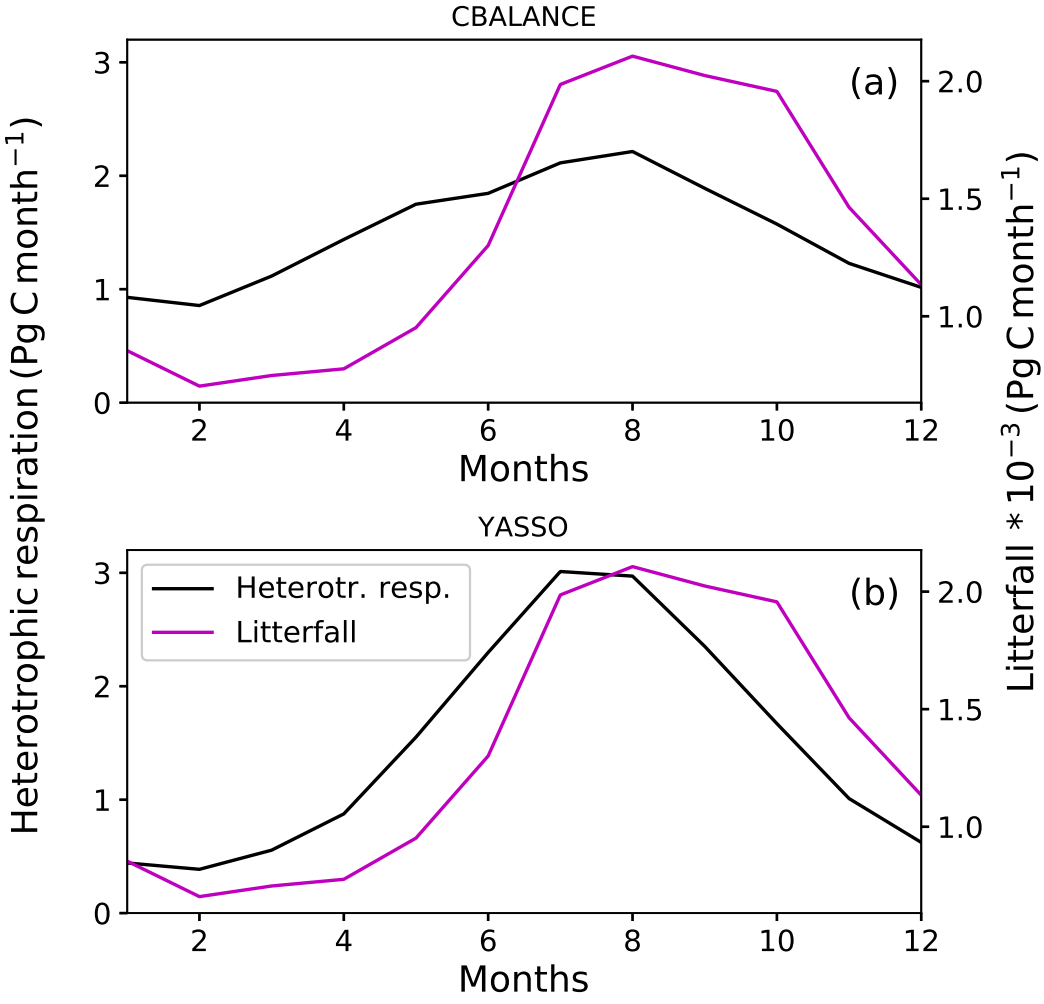

Figure S8. The heterotrophic respiration by the CBALANCE (a) and YASSO (b) models in the latitudinal zone 30°-60° in the Northern Hemisphere together with the litterfall.

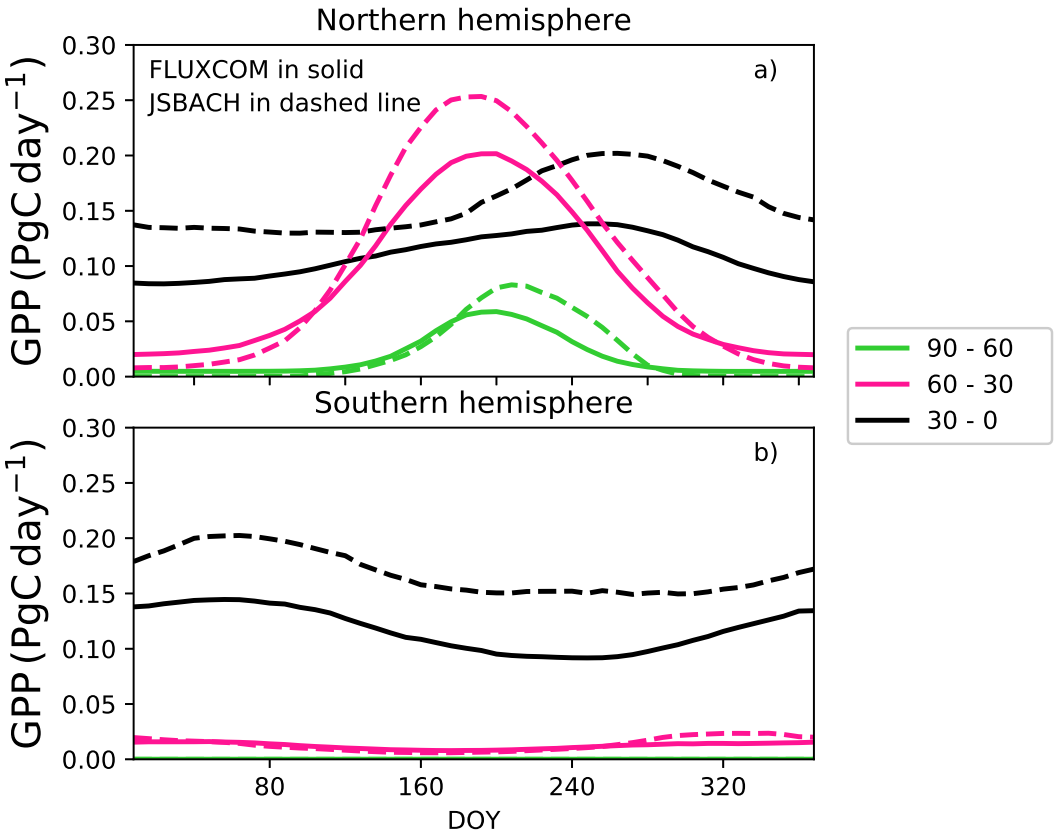

Figure S9. The seasonal cycle of GPP, which is independent of the soil module, for different latitudinal zones in northern (a) and southern (b) hemispheres. The FLUXCOM is in solid line, the JSBACH result in dashed line.

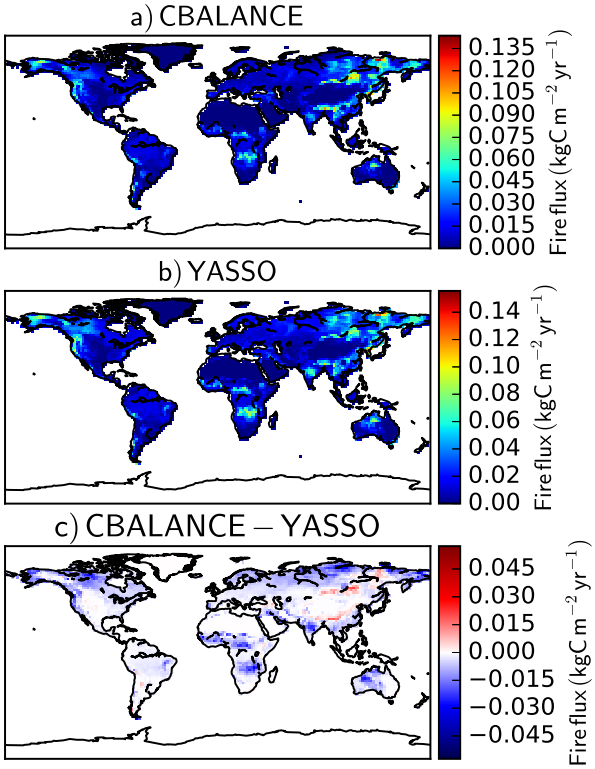

Figure S10. The global map of averaged annual fire fluxes by CBALANCE (a), YASSO (b) and their difference (c).

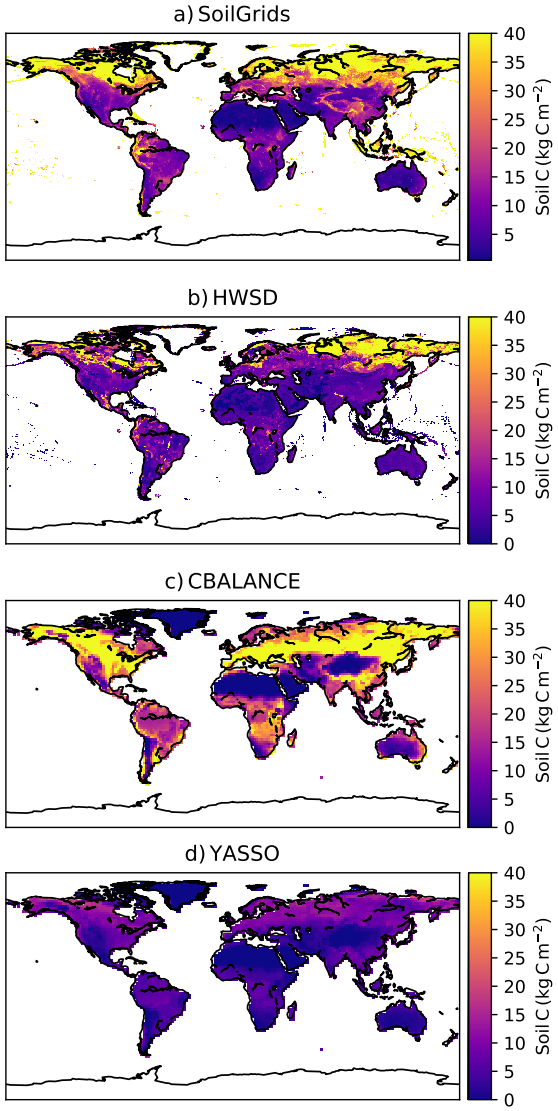

Figure S11. Map of organic soil carbon from datasets SoilGrids (a) and HWSD (b) and the model results from the CBALANCE model (c) and the YASSO model (d).

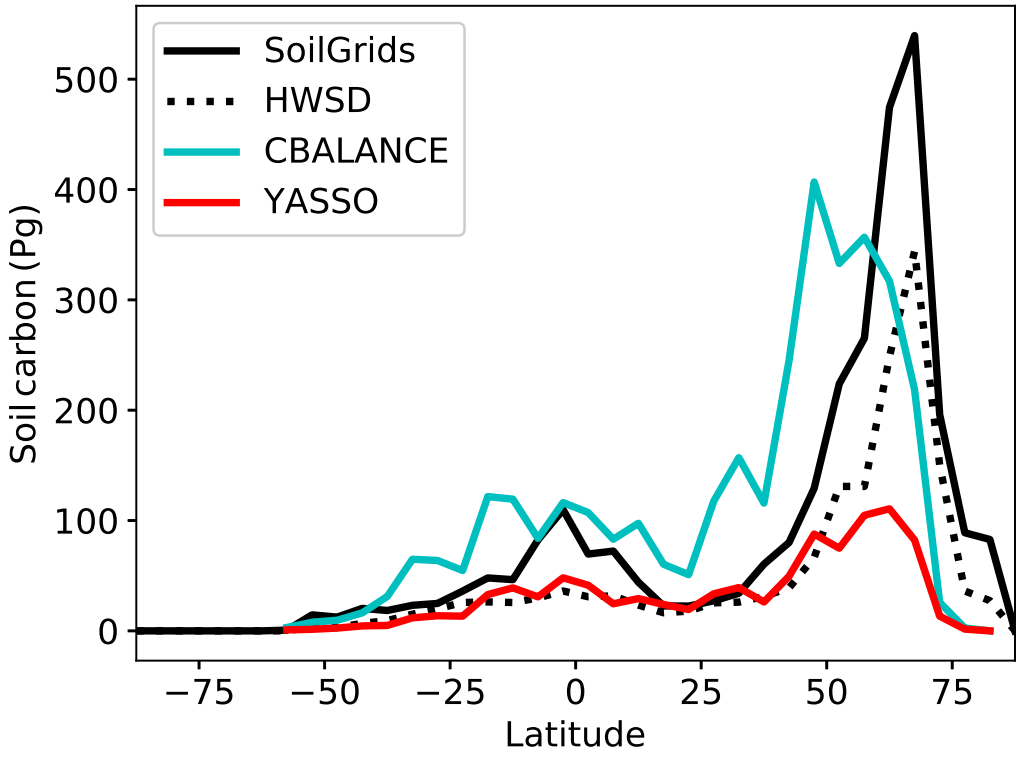

Figure S12. The latitudinal gradient of soil carbon down to one meter depth in five degree latitudinal bands from data products SoilGrids (solid line) and Harmonized World Soil Database (HWSD) (dashed line) with the model estimates from the CBALANCE (in cyan) and YASSO (in red) models.

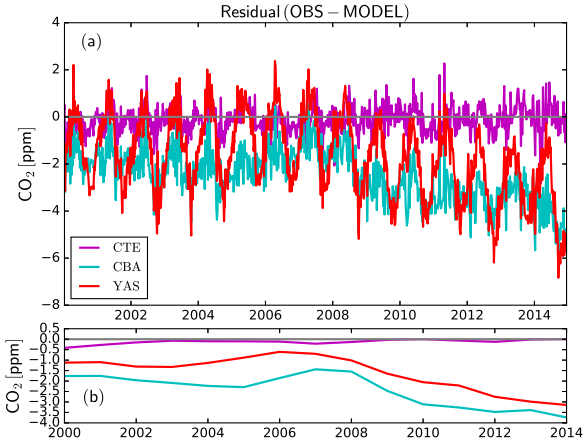

Figure S13. The residual between the observed and modelled CO_2 molar fraction (in ppm) at Mauna Loa between 2000 and 2014. The residual between observations and CarbonTracker Europe 2016 (CTE) in magenta, between observations and CBALANCE (CBA) in cyan and between observations and YASSO (YAS) in red. The values are given for the whole flask observational time series (a) and yearly averages (b).

Table S1. The annual fossil fuel and ocean fluxes from CarbonTracker Europe (CTE2016).

Year	Fossil fuel (PgCyr^{-1})	Ocean (PgCyr^{-1})
2001	6.97	-1.60
2002	7.07	-1.31
2003	7.47	-2.16
2004	7.87	-2.33
2005	8.22	-2.27
2006	8.52	-2.72
2007	8.77	-2.46
2008	8.98	-2.49
2009	8.86	-2.04
2010	9.20	-2.70
2011	9.53	-2.49
2012	9.71	-2.73
2013	9.81	-2.61
2014	9.88	-2.64

Table S2. The r^2 values and the root mean square error (RMSE) between the data-based soil carbon stock estimates and the model estimates from CBA and YAS calculated from latitudinal gradients.

	r^2	RMSE (PgC)
SoilGrids vs CBA	0.37	108
HWSD vs. CBA	0.31	113
SoilGrids vs. YAS	0.58	125
HWSD vs. YAS	0.50	62.6

Table S3. The seasonal cycle amplitudes, carbon uptake periods and Pearson correlation coefficients for the four Global Atmosphere Watch sites.

Variable (Unit)	Alert	Pallas	Niwot Ridge	Mauna Loa
Seasonal cycle amplitude (ppm)				
Obs.	16.2	19.3	8.7	7.1
CTE	16.1	17.7	8.1	6.6
CBA	23.8	27.8	8.4	6.2
YAS	15.5	19.2	3.7	3.6
Carbon uptake period (days)				
Obs.	142	151	180	161
CTE	144	150	177	162
CBA	141	150	179	157
YAS	140	155	186	145
r^2 (-)				
CTE	0.99	0.99	0.95	0.99
CBA	0.99	0.99	0.91	0.99
YAS	0.81	0.83	0.80	0.94

Table S4. The SCAs and Pearson correlation coefficients for the TransCom (TC) regions for the GOSAT observations, the CBALANCE (CBA) model and the YASSO (YAS) model.

Variable (unit)	GOSAT	CBA	YAS
SCA (ppm)			
TC=1	11.6	14.5	10.4
TC=2	6.4	5.8	2.8
TC=3	4.6	5.0	5.4
TC=4	1.9	2.8	3.1
TC=5	5.4	5.2	2.9
TC=6	2.8	2.5	2.3
TC=7	11.2	12.4	7.4
TC=8	6.8	5.0	2.2
TC=9	5.5	3.9	3.9
TC=10	1.4	1.5	1.5
TC=11	4.1	4.5	3.5
r^2 (-)			
TC=1	-	0.94	0.75
TC=2	-	0.90	0.83
TC=3	-	0.81	0.49
TC=4	-	0.34	0.00
TC=5	-	0.51	0.05
TC=6	-	0.83	0.80
TC=7	-	0.89	0.80
TC=8	-	0.86	0.80
TC=9	-	0.72	0.66
TC=10	-	0.88	0.86
TC=11	-	0.96	0.96